



## **Comparison of the freezing behavior of two liverwort species – *Conocephalum salebrosum* and *Marchantia polymorpha* subsp. *ruderalis***

Authors: Schott, Rena T., Nebel, Martin, and Roth-Nebelsick, Anita

Source: Lindbergia, 2021(1)

Published By: Dutch Bryological and Lichenological Society and Nordic Bryological Society

URL: <https://doi.org/10.25227/linbg.01135>

---

BioOne Complete ([complete.BioOne.org](https://complete.BioOne.org)) is a full-text database of 200 subscribed and open-access titles in the biological, ecological, and environmental sciences published by nonprofit societies, associations, museums, institutions, and presses.

Your use of this PDF, the BioOne Complete website, and all posted and associated content indicates your acceptance of BioOne's Terms of Use, available at [www.bioone.org/terms-of-use](https://www.bioone.org/terms-of-use).

Usage of BioOne Complete content is strictly limited to personal, educational, and non - commercial use. Commercial inquiries or rights and permissions requests should be directed to the individual publisher as copyright holder.

---

BioOne sees sustainable scholarly publishing as an inherently collaborative enterprise connecting authors, nonprofit publishers, academic institutions, research libraries, and research funders in the common goal of maximizing access to critical research.

# Comparison of the freezing behavior of two liverwort species – *Conocephalum salebrosum* and *Marchantia polymorpha* subsp. *ruderalis*

Rena T. Schott, Martin Nebel and Anita Roth-Nebelsick

R. T. Schott ✉ (rena.schott@smns-bw.de) and A. Roth-Nebelsick, State Museum of Natural History Stuttgart, Stuttgart, Germany. – M. Nebel, Nees Inst. for Biodiversity of Plants, Bonn, Germany.

Extracellular ice formation as a dehydrating agent is generally acknowledged as an important element of freezing avoidance in frost hardy plants, preventing the development of lethal ice crystals within living cells. While many reports on extracellular ice formation do exist for vascular plants, not much is known on ice formation for liverworts. In this study, ice formation was studied for two liverwort species occurring in climate zones with winter freezing, *Conocephalum salebrosum* and *Marchantia polymorpha* L. subsp. *ruderalis*, together with taxon-specific ice nucleating temperature and seasonal concentration of ice nucleating agents. Samples were collected in late autumn from various sites in south west Germany. Afterwards the collected liverwort specimen were cultivated and acclimated in pots in the inner courtyard of the State Museum of Natural History Stuttgart, Germany. Ice formation was observed in the environmental scanning electron microscope (ESEM) within the air chambers of both species, with ice crystals growing out of the air chamber pores, as well as random ice crystal formation on various sites on the ventral side for both taxa. The growing ice sheets led to dehydration particularly of the parenchymatous cells. For both taxa, the observations support the relevance of extracellular ice formation for surviving freezing conditions but the experiments also indicate a better adaptation of *C. salebrosum* to frost.

Keywords: ice formation, SEM, ESEM, ice nucleation, frost hardiness

There are different strategies and mechanisms in frost hardy plants to survive freezing temperatures in seasonal climates. Dehydration of living cells by extracellular ice formation is a common phenomenon in frost hardy vascular plants and can be found in many different tissues, such as petioles (Prillieux 1869, McCully et al. 2004), stems (Schaffner 1908, Schott et al. 2017), leaves (Ball et al. 2004) and twigs (Schott and Roth-Nebelsick 2018). After formation of ice in intercellular air spaces, the ice acts as dehydrating agent due to its low water potential (Guy 1990). Formation of ice in plants, including mosses and liverworts, is triggered by heterogeneous nucleation (Sakai and Larcher 1987, Gusta and Wisniewski 2013, Moffett 2015). Different kinds of ice nucleating agents were found, such as bacteria, fungi or macromolecules (Lindow et al. 1978, Wisniewski et al. 2002) and can also be produced by the plants themselves (Brush et al. 1994). Also, formation of plant-internal ice can be nucle-

ated by external ice which spreads into the plant through, for example, stomata (Wisniewski and Fuller 1999). The concentration of internal ice nucleating agents in vascular plants was demonstrated to show seasonal changes (Kishimoto et al. 2014a, b, Schott and Roth-Nebelsick 2018).

For cryptogams, much less information is available on plant internal ice formation or the activity of ice nucleating agents. For *Ceratodon purpureus*, a world-wide distributed moss, it was shown that this moss species avoids internal freezing by rapid dehydration (Lenné et al. 2011). To the authors' knowledge, not many researchers focused on the extracellular freezing of liverworts (Moffett 2015). The focus of this contribution is on freezing processes in liverworts and possible extracellular ice formation. Both dioicous species (*Conocephalum salebrosum* Szweyk., Buczk. and Odrzyk; *Marchantia polymorpha* L. subsp. *ruderalis* Bischl. and Boisselier) as members of the complex thalloid liverworts (Paton 2014) show a highly developed thallus with a costa, an upper and lower epidermis, several layers of parenchymal cells, air chambers, oil bodies in separate cells without chloroplasts, conducting tissue, ventral scales and dimorphic rhizoids, both smooth and with tubercles on the walls. As further described below, the considered taxa differ with respect to

This work is licensed under the terms of a Creative Commons Attribution 4.0 International License (CC-BY) <<http://creativecommons.org/licenses/by/4.0/>>. The license permits use, distribution and reproduction in any medium, provided the original work is properly cited.

distribution and habitat, and this may possibly imply different responses to freezing temperatures.

Within this contribution, freezing behavior and related structural details of *C. salebrosum* and *M. polymorpha* subsp. *ruderalis* were studied with a scanning electron microscope (SEM) and an environmental scanning electron microscope (ESEM). Additionally interspecific ice nucleation temperature (INT) and ice nucleation activity (INA) were determined, as well as the water content. The INT median ( $T_{INT}$ ) as well as the median cumulative ice nucleation per gram fresh weight or per water volume provide species-specific information of ice nucleation activity at defined temperatures, including seasonal changes. Both parameters indicate how readily ice forms under subzero conditions. Therefore the difference between season-specific data (winter and spring) of naturally acclimated material is expected to indicate, firstly, an acclimation to winter freezing and, secondly, the loss of this acclimation during spring. In frost hardy species, freezing is usually promoted. These values are important for analysis of frost hardiness and the comparison of different species, tissues, ontogenetic changes and seasonal differences with respect to frost resistance and susceptibility to freezing.

## Material and methods

### Plant material

*Conocephalum salebrosum* is a holarctic liverwort species (Szweykowski et al. 2005) with a distribution known so far to comprise Europe, including Scandinavia, East Asia and North America, reaching up to high latitudes. *C. salebrosum* occurs in big patches on mildly acid to basic, often humus rich soils on moist banks, rocks and stonework or on thin soil on limestone, typically on deeply shaded sites.

*Marchantia polymorpha* subsp. *ruderalis* as a classic research plant (Shimamura 2016) is distributed in temperate regions in Europe, Macaronesia, North America, Asia and introduced to South Africa. Growing on a variety of substrates, from moist to rather dry loamy, gravelly or peaty,

acid or basic and often nutrient-rich soils, *M. polymorpha* subsp. *ruderalis* is a horticultural weed in exposed or shaded man-made habitats. This species is also a characteristic pioneer on gravel, paths, waste ground and bonfire sites, in gardens, parks and nurseries, also in and around glasshouses occasionally in woodlands and beside streams. The appearance is often sporadic (Paton 2014).

To the authors' knowledge, no explicit data are available, a certain difference in freezing tolerance might be expected from the different distribution of both species. All species sampled were collected in late autumn in south west Germany (*Conocephalum salebrosum*: Erms Valley (48°26'35.844"N, 9°27'43.523"E); *Marchantia polymorpha* subsp. *ruderalis* in green houses of Hohenheim Gardens (48°42'34.272"N, 9°12'34.164"E) and breeder Hummel (48°48'23.616"N, 9°6'56.087"E)). Afterwards samples were cultivated and acclimated in pots in the inner courtyard of the State Museum of Natural History Stuttgart, Germany (48°47'35.909"N, 9°11'25.224"E).

During winter, the cultivated material was used to prepare frozen samples as well as for the freezing experiments in the ESEM and to determine the ice nucleation temperature. After being naturally exposed to temperatures < 5°C for some days, including at least three days below 0°C, the cultivated material was naturally acclimated to lower (winter) temperatures. Otherwise, with un-acclimated material, freezing experiments may lead to artifacts (Ball et al. 2004). The remaining cultivated plants in the pots in the inner courtyard were also used for the ice nucleation temperature determination in spring after de-acclimation. De-acclimation occurred at temperatures above 5°C. During the time of the study, it was sufficiently humid so that the regularly checked pot substrate did not need any additional watering. Table 1 gives an overview of the used samples in each experiment.

### Determination of ice nucleation temperature and water content

For comparison of the species-specific ice nucleation temperature, for the acclimated as well as the de-acclimated state, measurements were conducted during winter and spring.

Table 1. Description of the samples used for the experiments (°C: degree Celsius).

Experiment	Natural acclimation	Season	Extra pre-treatment	Collection site	Species
Determination of ice nucleation temperature	yes	winter	stored overnight at +3°C	Erms Valley	<i>C. salebrosum</i>
Determination of ice nucleation temperature	yes	winter	stored overnight at +3°C	Hohenheimer Gardens/breeder Hummel	<i>M. polymorpha</i>
Determination of ice nucleation temperature	yes	spring	none	Erms Valley	<i>C. salebrosum</i>
Determination of ice nucleation temperature	yes	spring	none	Hohenheimer Gardens/breeder Hummel	<i>M. polymorpha</i>
Determination of water content	yes	winter	none	Erms Valley	<i>C. salebrosum</i>
Determination of water content	yes	winter	none	Hohenheimer Gardens/breeder Hummel	<i>M. polymorpha</i>
SEM	yes	winter	stored 3 days at -10°C	Erms Valley	<i>C. salebrosum</i>
SEM	yes	winter	stored 3 days at -10°C	Hohenheimer Gardens/breeder Hummel	<i>M. polymorpha</i>
SEM	yes	winter	none	Erms Valley	<i>C. salebrosum</i>
SEM	yes	winter	none	Hohenheimer Gardens/breeder Hummel	<i>M. polymorpha</i>
ESEM	yes	winter	none	Erms Valley	<i>C. salebrosum</i>
ESEM	yes	winter	none	Hohenheimer Gardens/breeder Hummel	<i>M. polymorpha</i>

Kishimoto et al. (2014a, b) devised a method to determine ice nucleation temperature (INT) which also provides the content of ice nucleating particles within a sample (ice nucleation activity – INA). In this contribution, a variation of the original method was applied, as described in Schott and Roth-Nebelsick (2018). The basic procedure is as follows. Firstly, 40 glass tubes containing 0.2 ml ultrapure (type 1) water were autoclaved at 121°C for 20 min as described by Kishimoto et al. (2014a, b). A sample of each species was brought into the laboratory and divided into 20 portions (weight of each portion: *C. salebrosum*: 32.3–66 mg; *M. polymorpha* subsp. *ruderalis*: 33.1–57.3 mg). Before the experiment, the ventral side of the liverwort samples were carefully cleaned with a razor blade to remove as much substrate as possible.

In winter, samples from completely frozen plants required a storage at a cold non-freezing temperature (+3°C) in a

custom-built freezer overnight before the INT experiment. The freezer, equipped with a triple glazed door and a temperature accuracy of  $\pm 1.2^\circ\text{C}$ , was also used for all freezing experiments. Each glass tube received one sample portion, meaning that one experiment included 20 replications for each species. The whole experiment was repeated each four times in winter and spring. For each measurement, eight glass tubes solely filled with autoclaved ultrapure (type 1) H<sub>2</sub>O served as control. To be sure that the ultrapure (type 1) H<sub>2</sub>O would not influence the results, the ice nucleation temperature of the water control was determined in a pre-experiment, with a result of  $-16.45^\circ\text{C} \pm \text{SE } 0.05$  (Schott and Roth-Nebelsick 2018).

All glass tubes, with and without tissue samples, were placed into the precooled (0°C) freezer. The samples were cooled down by 1° every 20 min while the already frozen tubes were counted during each step. To support reliable

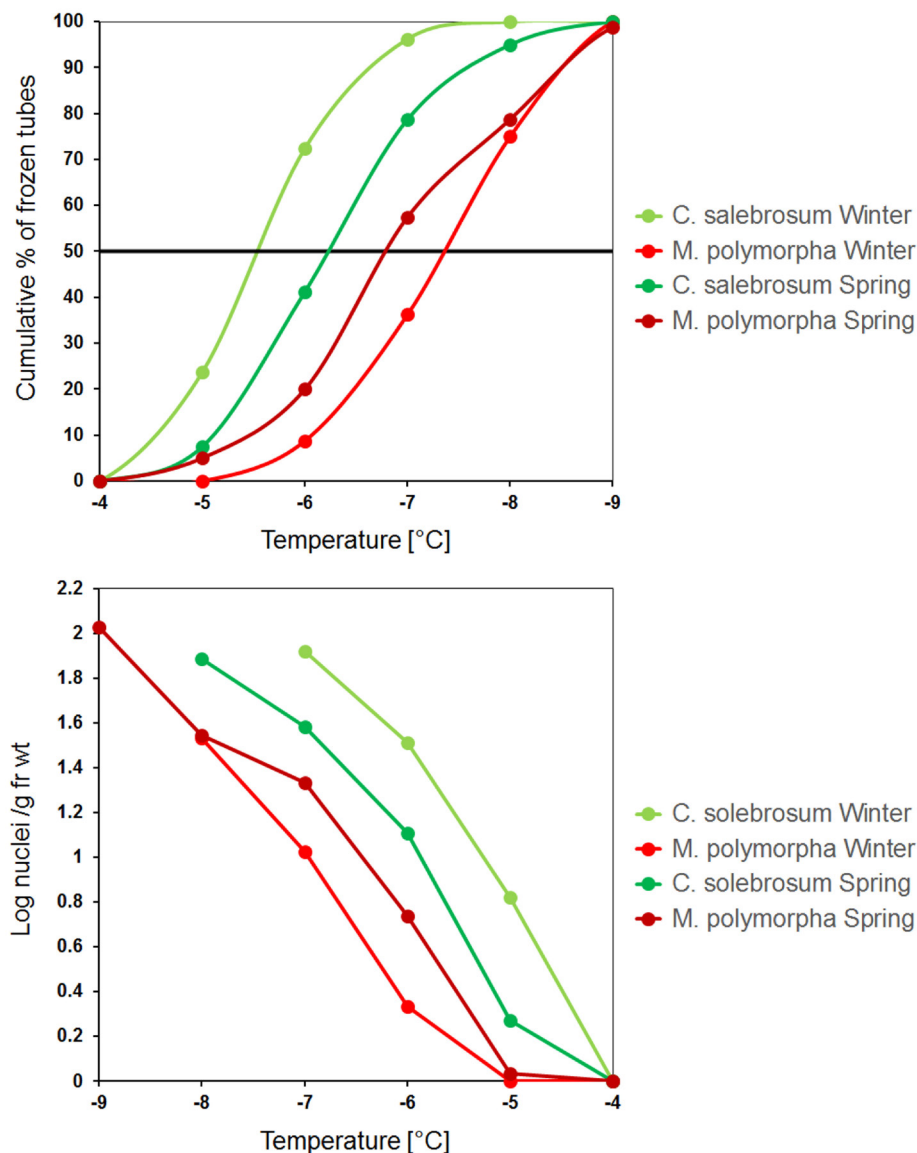


Figure 1. (A) Distribution of ice nucleation activity (INA) shown as cumulative percentage of frozen glass tubes (n=20). (B) Cumulative ice nucleation showing  $K'(T)$  (ice nuclei per g fresh weight) for *C. salebrosum* and *M. polymorpha* subsp. *ruderalis* in winter and spring.

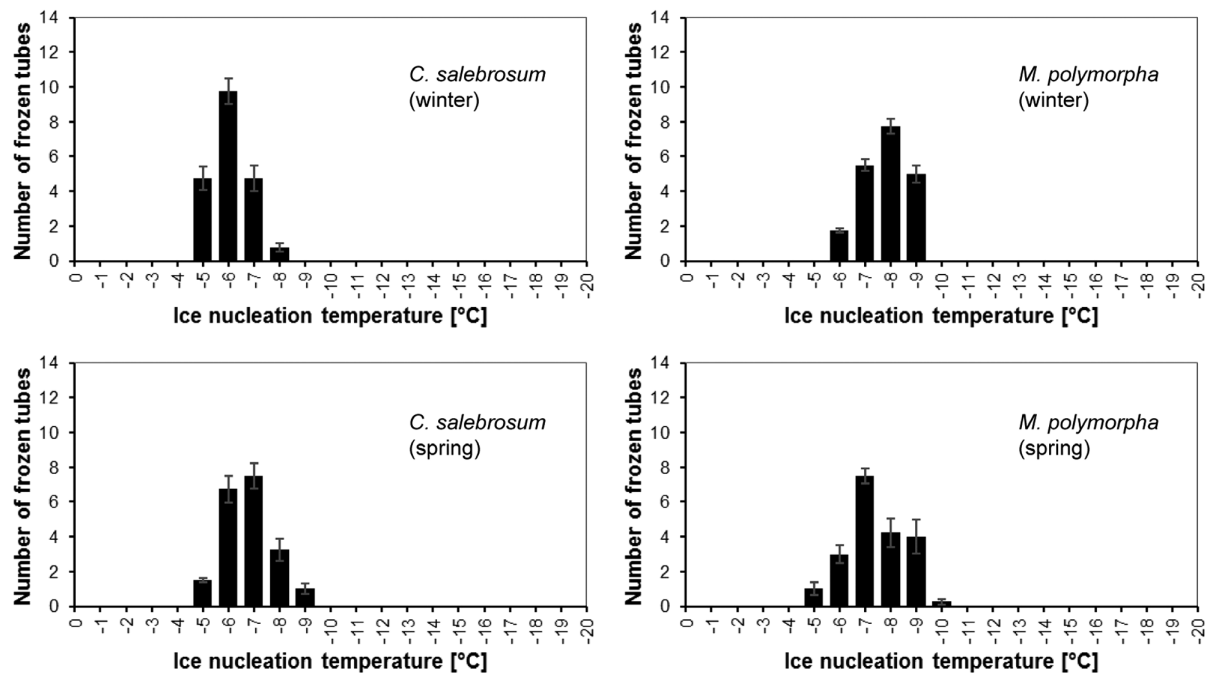


Figure 2. Distribution of ice nucleation activity of *C. salebrosum* and *M. polymorpha* subsp. *ruderalis* in glass tubes (n=20) in winter and spring.

identification of frozen samples, the glass tubes were placed onto a small wooden shelf with a black background. This arrangement provided sufficient contrast between sample and background to observe ice crystal growth. The whole experiment was repeated each four times (as described by Kishimoto et al. 2014a, b). A pre-experiment determined the minimum weight required for each sample. In pre-experiments, the temperature development of the shelf in the freezer was measured to exclude any bias by the equipment. The experimental procedure applied in this study was a in following explained variation of the original method, as described in Schott and Roth-Nebelsick (2018), because the limited amount of available cultivated liverworts required a reduction of the water volume from originally 0.5 ml to 0.2 ml and also reduction of replications from 40 to 20.

The results provide the median  $T_{INT}$  of ice nucleating temperature and the ice nuclei concentration per g fresh weight, which provide species-specific values as well as an indication for the degree of acclimation (Kishimoto et al. 2014b). The results of the calculation of the cumulative concentration (per unit mass of the sample) of ice nuclei that were active at all temperatures warmer than  $T$  ( $K'(T)$ ) (Vali 1995) can best be shown and compared with literature results on the basis of a log 10 ( $K'(T)$ ) graph. The number of active ice nuclei indicate specific freezing events.

For the determination of the water content, 10 samples from each species were weight in the fresh state, and then dried to constant weight in a drying cabinet.

## Microscopic a nalysis

### SEM

For observation of the structure of the liverworts before freezing, freshly cut samples were transferred into pure methanol for 10 min, then into pure ethanol for 30 min. The last step was repeated. Afterwards the samples were critical point dried (Leica EM CPD300). The procedure was described by Talbot and White (2013) and largely prevents deformation of living plant tissues. The dried samples were mounted on SEM stubs by using special adhesive tape and sputtered with gold palladium (sputter layer thickness 6 nm) before examination in the SEM (ZeissEVO LS 15).

To study plant structure after freezing, samples of both species were cooled in the custom-built freezer. Temperature was reduced from 0°C to -10°C with a cooling rate of 2° h<sup>-1</sup>, a frequent cooling rate under natural conditions (Steffen et al. 1989). After reaching -10°C plants were stored within the freezer for ~ 3 days before they were prepared together with the fresh samples for SEM.

Table 2. Results of ice nucleation temperature and median of ice nuclei active at -7°C for *C. salebrosum* and *M. polymorpha* subsp. *ruderalis* (°C: degree Celsius).

Species	<i>C. salebrosum</i>	<i>M. polymorpha</i> subsp. <i>ruderalis</i>	<i>C. salebrosum</i>	<i>M. polymorpha</i> subsp. <i>ruderalis</i>
Season	winter (Januar)	winter (Januar)	spring (April)	spring (April)
Median INT [°C] ± SE (n=4)	-5.54 ± 0.44	-7.35 ± 0.47	-6.23 ± 0.45	-6.8 ± 0.46
Median of ice nuclei active at -7°C	83	11	39	22



Table 3. Water content and standard deviation (SD) in winter for 10 samples in 2 repetitions each of *C. salebrosum* and *M. polymorpha* subsp. *ruderalis*.

Species	<i>C. salebrosum</i>	<i>M. polymorpha</i> subsp. <i>ruderalis</i>
Water content and SD in winter	78.97% ± 2.48	76.50% ± 3.08

ESEM

With the ESEM, allowing for maintaining controlled levels of humidity and temperature inside the sample chamber, it is possible to observe samples in a native state during freezing. For the ESEM freezing experiments with fresh, unfrozen and untreated native samples, the same SEM equipment was used as described above, but run in ESEM mode, including a precooled peltier at 0°C, a pressure of ~ 259 Pa and a humidity of ~90%. The temperature was lowered to -10°C.

For this study another add-on regulating the temperature inside the analysis chamber was used for the experiments. Appearance of ice crystals and their development

was detected and observed. The ESEM conditions suitable for initiating and observing freezing processes were selected according to Konrad et al. (2019).

Results

Comparison of the ice nucleation activity

INT data of *Marchantia polymorpha* subsp. *ruderalis* showed smaller differences between winter and spring samples than *Conosephalum salebrosum* (Fig. 1A) with fewer ice nuclei active at the same temperature, and particularly so for the winter samples (Fig. 1B). Both species show a broader distribution of freezing temperatures in spring (Fig. 2). During winter, the median INT was lower for *M. polymorpha* subsp. *ruderalis* (-7.35°C ± 0.47) than for *C. salebrosum* (-5.54 ± 0.44) (Table 2). In spring, no significant differences between *M. polymorpha* subsp. *ruderalis* (-6.8°C ± 0.46) and *C. salebrosum* (6.23°C ± 0.45) could be detected. The median for active ice nuclei (at -7°C) for *C. salebrosum* was sub-

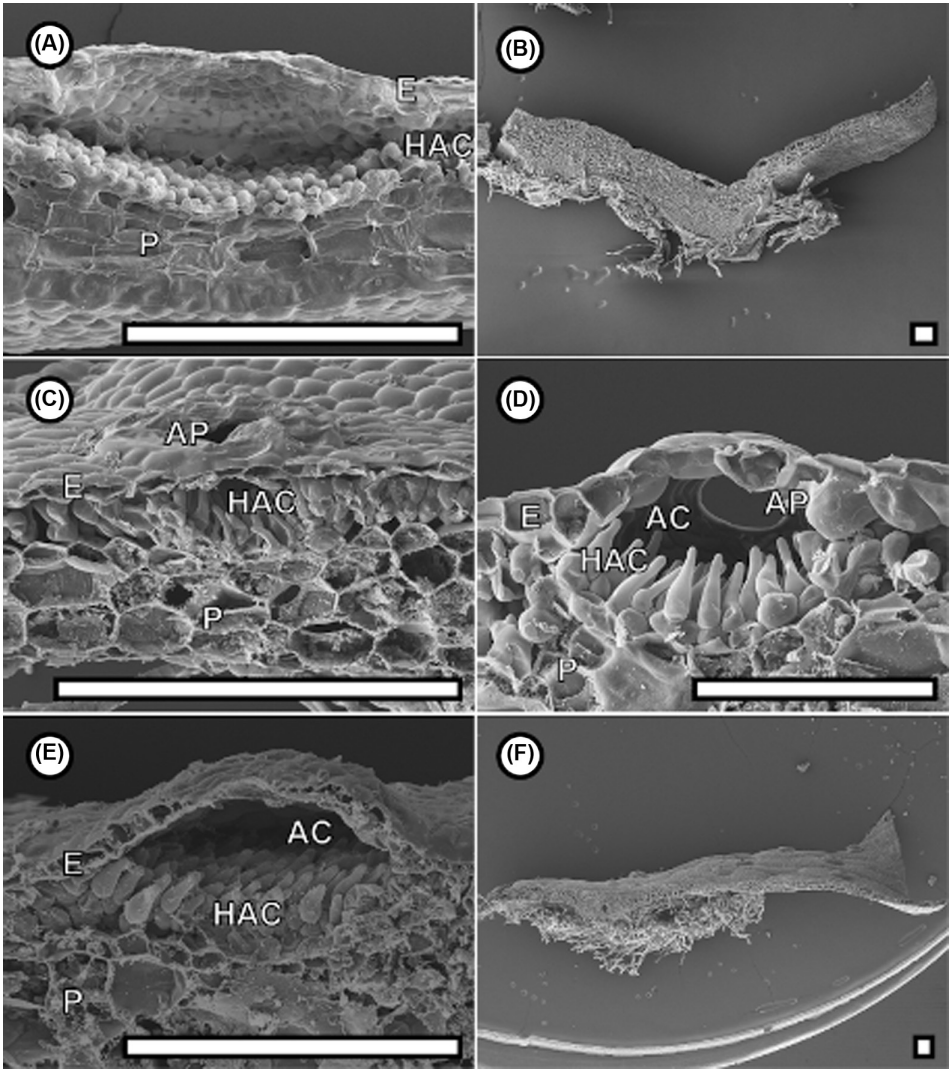


Figure 3. Cross sections of freshly (A–D) and frozen (E–F) dried *C. salebrosum* (SEM). AC: air chamber; AP: air pores; E: epidermis; HAC: hyaline apical cell; P: parenchyma. Scale bars: 200 μm.

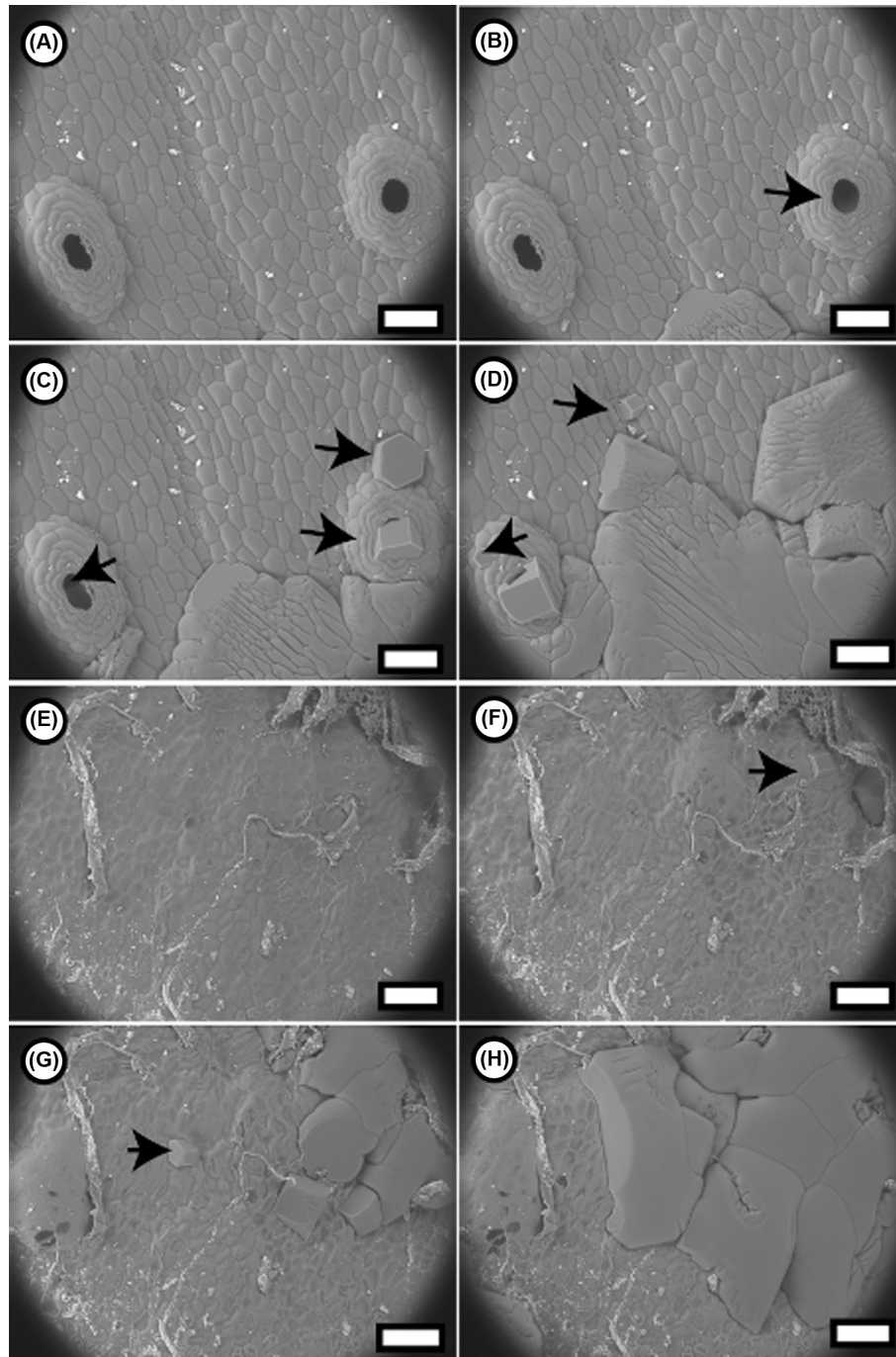


Figure 4. ESEM images of different steps during artificial freezing events ( $-10^{\circ}\text{C}$ ) with a humidity of 90% and 259 Pa. (A–D) *C. salebrosum* upper surface. (E–H) *C. salebrosum* lower surface. Black arrows highlight the ice crystal growth. Scale bars: 100  $\mu\text{m}$ .

stantially lower in spring compared to winter. Both species showed a quite similar water content (Table 3).

### Microscopic observations

#### *Conocephalum salebrosum*

When comparing cross sections of samples of *C. salebrosum* prepared from the unfrozen and frozen state (Fig. 3), a slight deformation of the epidermis and the parenchymatous tissue was visible for the frozen samples. The chlorenchyma within

the air chamber as well as the hyaline apical cells below the air chamber pores show nearly no deformation (Fig. 3C–E). The parenchyma cells adjacent to the chlorenchyma appear to be smaller than the rest of the parenchyma.

Observation of the freezing process of *C. salebrosum* in ESEM reveals a quite interesting pattern (Fig. 4). During cooling, ice crystals appear at the entrance of the air chamber pore, originating from tissue water (Fig. 4B–D). Next to these growing ice crystals, ice can occur around the external base of the air pores (Fig. 4C–D). Ice crystals can also form

above the junctions between air chamber and epidermis (Fig. 4D). Finally, an ice sheet forms with additional ice possibly originating at other sites of the thallus (Fig. 4D). On the ventral side of the thallus, ice forms randomly at different sites and starts to grow and merge until it covers the surface completely (Fig. 4E–H).

#### *Marchantia polymorpha* subsp. *ruderalis*

The SEM cross sections of *M. polymorpha* subsp. *ruderalis* display smaller epidermis cells and large parenchyma cells in the central region of the thallus, close to the chlorenchyma cells, while parenchymatous cells close to the ventral side are smaller (Fig. 5). Although preparation of the frozen samples was difficult because the frozen tissue disintegrated stronger compared to *C. salebrosum*, the SEM images indicate a shrinkage of tissue, particularly for the larger parenchyma cells (Fig. 6E–F).

During the freezing process in the ESEM, ice crystals grow mainly out of the air chamber pores (Fig. 6B–D), similar to *C. salebrosum*. On the ventral side, ice formation started randomly at many locations on the surface and finally covered the ventral surface (Fig. 6F–H).

#### Interspecific comparison

For both taxa, SEM images indicate shrinkage of the frozen samples compared to the unfrozen state, and particularly so for the larger parenchyma cells. It also appears that freezing-induced shrinkage was higher in *M. polymorpha* subsp. *ruderalis*, compared to *C. salebrosum*.

The ESEM experiments highlighted extracellular freezing on the surface (Fig. 4, 6, 7) of both sides for the two species. On the dorsal side, ice crystals grew rapidly out of air chamber pores in both taxa. Particularly in *C. salebrosum*, the dorsal side was finally covered by an ice sheet.

In both species, an ice cover developed swiftly on the ventral sides, starting from random ice crystal formation at many sites.

#### Discussion

Results of INT and INA experiments support the notion of a better adaptation of *Conocephalum salebrosum* to frost, as compared to *Marchantia polymorpha* subsp. *ruderalis*, because freezing appears to be slightly promoted in *C. salebrosum*,

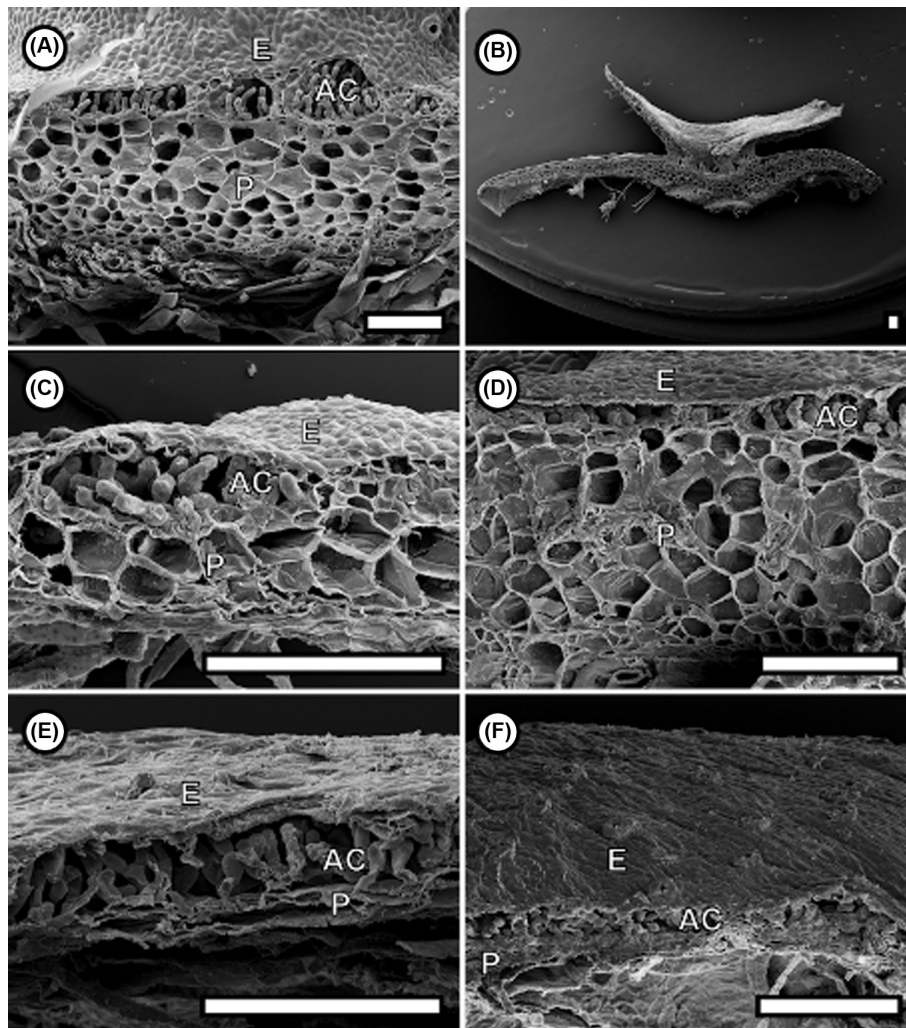


Figure 5. Cross sections of freshly (A–D) and frozen (E–F) dried *M. polymorpha* subsp. *ruderalis* (SEM). AC: air chamber; E: epidermis; P: parenchyma. Scale bars: 200  $\mu$ m.



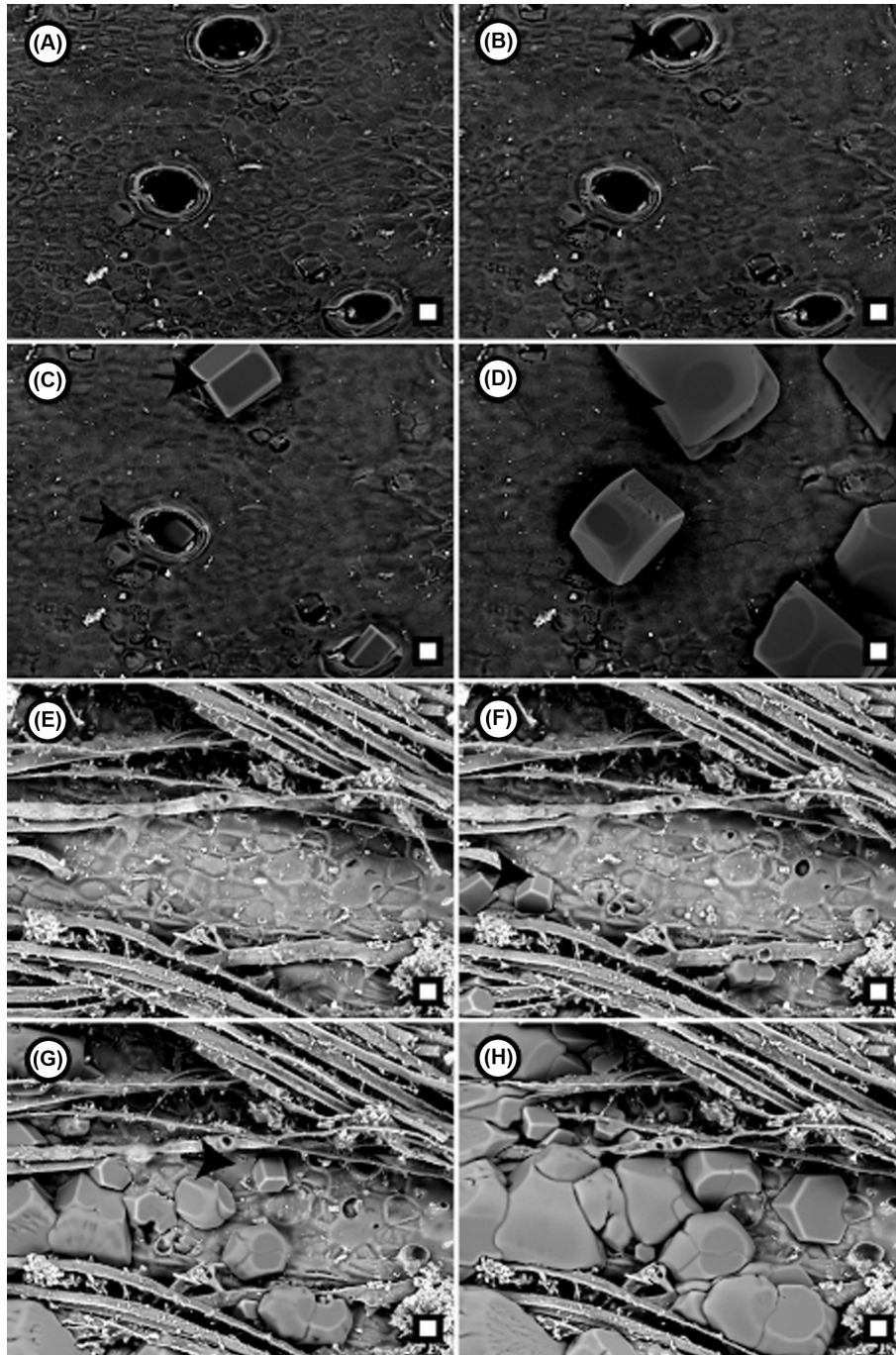


Figure 6. ESEM images of different steps during artificial freezing events ( $-10^{\circ}\text{C}$ ) with a humidity of 90% and 259 Pa. (A–D) *M. polymorpha* subsp. *ruderalis* upper surface. (E–H) *M. polymorpha* subsp. *ruderalis* lower surface. Black arrows highlight important ice formations. Scale bars: 20  $\mu\text{m}$ .

particularly during the winter (Kishimoto et al. 2014a, b, Schott and Roth-Nebelsick 2018). This difference may be related to the different distribution of both taxa, indicating the ability of *C. salebrosum* to cope better with harsher habitats, such as in regions with high elevation. However, this is quite conjectural at the moment.

Although internal ice formation could not be observed with the methods applied in this study, evidence for plant-internal and intercellular ice formation could be found, because ice crystals grew directly out of the air chambers, and also on the ventral thallus side. Ice growing out of air

chambers therefore originates from water of internal tissues, which fed ice crystal growth, thereby dehydrating the cells. After a while a massive dorsal ice sheet was formed. The air chambers as preferential sides of ice crystal formation can be explained with the presence of a quite watertight cuticle on the epidermis in Marchantiales, including hydrophobic ledges preventing water to enter the pores (Schönherr and Ziegler 1975). In *C. salebrosum* a strong water loss of internal tissues is indicated. Possibly, the origin of the massive sheet was the hyaline thallus margin, or the junctions between air chamber walls and epidermis, which form distinct furrows

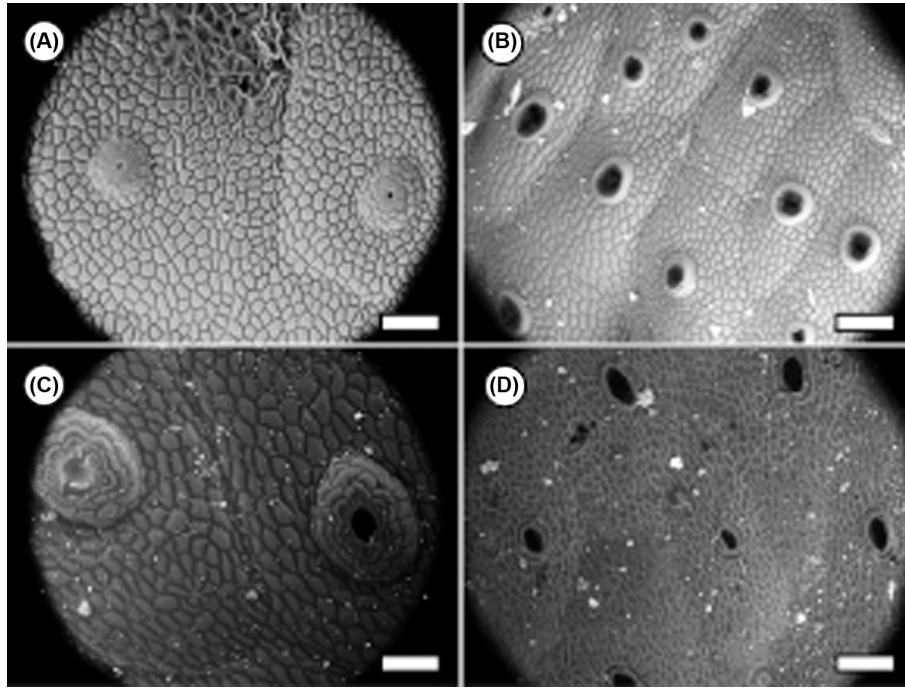


Figure 7. upper surface of current year (A) and older (C) *C. salebrosum* and of current year (B) and older (D) *M. polymorpha* subsp. *ruderalis* (ESEM) with a humidity of 80% and ~ 700 Pa and a peltier temperature of 5°C. Scale bars: 100 µm.

in this taxon (Szweykowski et al. 2005). However, it was not possible within these observations to detect the water source for the ice sheets.

In contrast to the dorsal site, ice started to form irregularly on the ventral sides of the thalli in both taxa, seemingly randomly at various spots, merging rapidly into ice sheets. This is consistent with the lack of a cuticle at the ventral sides and therefore the absence of a water barrier. Parallel to the ice growth on both sides of the thallus, internal tissues became dehydrated, and particularly so parenchymatous cells. Since the thalli are quite shallow, the ice bodies on both thallus sides probably caused dehydration of the internal tissues. The chlorenchymatous tissue as well as – in *C. salebrosum* – the flask-shaped hyaline cells did not show considerable shrinkage. Possibly, these cells show a higher mechanical stiffness. As described by Konrad et al. (2019), water loss due to an adjacent ice body decreases with increasing cell wall stiffness. When layers of stiffer cells are located besides ‘softer’ cell layers, then water will be drawn preferentially from the softer cells towards ice bodies which then grow on expense of these cells (Konrad et al. 2019). Increasing dehydration leads at first to rising solute concentration within the cells and therefore to a further decreasing freezing point. Finally, cells may dehydrate strongly.

It is therefore possible that the chlorenchymatous cells of *C. salebrosum* and *M. polymorpha* subsp. *ruderalis* are mechanically more stable than the parenchymatous cells. When layers of stiffer cells are located besides ‘softer’ cell layers, then water will be drawn preferentially from the softer cells towards ice bodies which then grow on expense of these cells (Konrad et al. 2019). Water is absorbed again by the cells upon thawing, as it can be observed usually for frost hardy plants with extracellular freezing (Niklas 1989, McCully et al. 2004, Roden et al. 2009). In the same

manner, melting water could then be used by the liverworts as a water reservoir in spring (Moffet 2015).

Although the observations refer to the specific environment of the cultivation site, the conditions met the characteristic requirements for cold acclimation.

**Acknowledgements** – The authors would like to thank Cristina Gasco Martin for her assistance with the SEM and ESEM.

**Funding** – This work has been funded by the German Research Foundation (DFG) as part of the Transregional Collaborative Research Centre (SFB/Transregio) 141 ‘Biological Design and Integrative Structures’/A01.

## References

- Ball, M. C., Canny, M. J., Huang, C. X. et al. 2004. Structural changes in acclimated and unacclimated leaves during freezing and thawing. – *Funct. Plant Biol.* 31: 29–40.
- Brush, R. A., Griffith, M. and Mlynarz, A. 1994. Characterization and quantification of intrinsic ice nucleators in winter rye *Secale cereale* leaves. – *Plant Physiol.* 104: 725–735.
- Gusta, L. V. and Wisniewski, M. 2013. Understanding plant cold hardiness: an opinion. – *Physiol. Plant.* 147: 4–14.
- Guy, C. L. 1990. Cold acclimation and freezing stress tolerance: role of protein metabolism. – *Annu. Rev. Plant Biol.* 41: 187–223.
- Kishimoto, T., Sekozawa, Y., Yamazaki, H. et al. 2014a. Seasonal changes in ice nucleation activity in blueberry stems and effects of cold treatments in vitro. – *Environ. Exp. Bot.* 106: 13–23.
- Kishimoto, T., Yamazaki, H., Saruwatari, A. et al. 2014b. High ice nucleation activity located in blueberry stem bark is linked to primary freeze initiation and adaptive freezing behaviour of the bark. – *AoB Plants* 6: plu044.
- Konrad, W., Schott, R. and Roth-Nebelsick, A. 2019. A model for extracellular freezing based on observations on *Equisetum hyemale*. – *J. Theor. Biol.* 478: 161–168.

- Lindow, S. E., Arny, D. C. and Upper, C. D. 1978. Distribution of ice nucleation-active bacteria on plants in nature. – *Appl. Environ. Microbiol.* 36: 831–838.
- Lenné, T., Bryant, G., Hocart, C. H. et al. 2011. Freeze avoidance: a dehydrating moss gathers no ice. – *Plant Cell Environ.* 33: 1–11.
- McCully, M. E., Canny, M. J. and Huang, C. X. 2004. The management of extracellular ice by petioles of frost-resistant herbaceous plants. – *Ann. Bot.* 94: 665–674.
- Moffet, B. F. 2015. Ice nucleation in mosses and liverworts. – *Lindbergia* 38: 14–16.
- Niklas, K. J. 1989. Extracellular freezing in *Equisetum hyemale*. – *Am. J. Bot.* 76: 627–631.
- Paton, J. A. 2014. The liverwort flora of the British Isles. – Brill Academic Pub.
- Prillieux, M. 1869. Effet de la gelée sur les plantes. Formation de glaçons dans les tissus des plantes. – *Bull. Soc. Bot. Fr.* 16: 140–152.
- Roden, J., Canny, M., Huang, C. et al. 2009. Frost tolerance and ice formation in *Pinus radiata* needles: ice management by the endodermis and transfusion tissues. – *Funct. Plant Biol.* 36: 180–189.
- Sakai, A. and Larcher, W. 1987. Frost survival of plants. Responses and adaptation to freezing stress. – Springer.
- Schaffner, J. H. 1908. The air cavities of equisetum as water reservoirs. – *Ohio Nat.* IX: 393–394.
- Schönherr, J. and Ziegler, H. 1975. Hydrophobic cuticular ledges prevent water entering the air pores of liverwort thalli. – *Planta* 124: 51–60.
- Schott, R. T. and Roth-Nebelsick, A. 2018. Ice nucleation in stems of trees and shrubs with different frost resistance. – *IAWA J.* 39: 177–190.
- Schott, R. T., Voigt, D. and Roth-Nebelsick, A. 2017. Extracellular ice management in the frost hardy horsetail *Equisetum hyemale* L. – *Flora* 234: 207–214.
- Shimamura, M. 2016. Marchantia polymorpha: taxonomy, phylogeny and morphology of a model system. – *Plant Cell Physiol.* 57: 230–256.
- Steffen, K. L., Arora, R. and Palta, J. P. 1989. Relative sensitivity of photosynthesis and respiration to freeze-thaw stress in herbaceous species: importance of realistic freeze-thaw protocols. – *Plant Physiol.* 89: 1372–1379.
- Szweykowski, J., Buczkowska, K., Odrzykoski, I. J. 2005. *Conocephalum salebrosum* (Marchantiopsida, Conocephalaceae) – a new Holarctic liverwort species. – *Plant Syst. Evol.* 253: 133–158.
- Talbot, M. J. and White, R. G. 2013. Methanol fixation of plant tissue for scanning electron microscopy improves preservation of tissue morphology and dimensions. – *Plant Methods* 9: 36.
- Vali, G. 1995. Principles of ice nucleation. – In: Lee, W. et al. (eds), *Biological ice nucleation and its applications*. APS Press, pp. 1–28.
- Wisniewski, M. and Fuller, M. 1999. Ice nucleation and deep supercooling in plants: new insights using infrared thermography. – In: Margesin, R. and Schinner, F. (eds), *Cold-adapted organisms: ecology, physiology, enzymology and molecular biology*. Springer, pp. 105–118.
- Wisniewski, M., Fuller, M., Glenn, D. M. et al. 2002. Extrinsic ice nucleation in plants. – In: Li, P. H. and Palva, E. T. (eds), *Plant cold hardiness*. Springer, pp. 211–221.